

Particle-rigid body dynamics model for terminal-sensitive submunition

Rui Guo, Rong-zhong Liu⁺, Zheng-jun Shi

School of Mechanical Engineering, Nanjing University of Science and Technology, Nanjing 210094, China

(Received October 6 2005, accepted November 1 2005)

Abstract. This paper deals with the dynamics characteristic of terminal-sensitive submunitions in missile. Firstly, the principle and working process of terminal-sensitive submunitions in missile are simply introduced, and the ballistic trajectory of the terminal-sensitive submunition is divided into two stages: freely falling stage, the deceleration and dispinning stage with decelerating parachute. Then, the forces and moments of the deceleration and dispinning stage is analyzed, on that basis, the particle-rigid body dynamics model is established. The model can provide the overall design and the stable scanning equipment design of the terminal-sensitive submunition with some helpful references, and can be used to the exterior ballistic of terminal-sensitive submunitions.

Key words: terminal-sensitive submunitions; particle-rigid body dynamics model; exterior ballistic.

1. Introduction

The terminal-sensitive submunition is a kind of sensing instrument initiation cluster bomb^{[2] [5]}. It is a new type of smart ammunition that applied advanced sensing instrument technology and EFP warhead technology to the cluster bombs .

When the guided missile flies to the scheduled region, the time fuze functions, and terminal-sensitive submunitions are projected from the cabin of the missile, then the battery activation device functions, the decelerating parachute is opened and charged. After certain time, when the speed of the submunition is decelerated the certain scope and the height is reduced the scheduled place, the decelerating parachute is discarded. At the same time, the rotational parachute is unfurled and begins to work under the aerodynamic influence. Finally, the projectile revolves and descends while it remains certain speed V and certain revolution speed ω . In the course of the steady decent, the sensing instrument scans and searches the targets within certain range. While armor vehicle is detected, the EFP warhead is detonated, the high speed EFP shots into the target and injures the target finally.

Because the terminal-sensitive submunition needs a steady working platform, the parachute-submunition system is needed to be decelerated before the rotational parachute is unfurled. The trajectory of the terminal-sensitive submunition is divided into two stages: from opening the cabin to the first time compartment projection is the freely falling stage, and from that to the second time compartment projection is the deceleration and dispinning stage.

When the cabin of the missile is opened and the terminal-sensitive submunitions are projected, the terminal-sensitive submunition freely falls period of time, the decelerating parachute is not opened in that stage. The motion of that period is called the free fall stage. When the terminal-sensitive submunition freely falls the scheduled height, the speed and the rotate speed is still much higher than the required parameters of the stable scanning. For providing the initial condition of the next stable scanning stage, the terminal-sensitive submunition needs to project the decelerating parachute's compartment and the decelerating parachute is opened at the same time. This is the first time compartment projection. Before the second time compartment projection, the speed of the submunition is decelerated the allowable range and the rotate speed is also decelerated the degree that the parachute cords of the rotational parachute are not winded. The motion of that period is called the deceleration and dispinning stage.

⁺ Corresponding author.
Email address: guoruid@163.com

Researches in the dynamics of parachute-submunition system, such as the particle dynamics model, the single rigid body dynamics model and the multi-rigid body dynamics model [2], [3], [4], [7].have been founded, and simulation based on MATLAB/Simulink has been introduced [1]. For farther study, the submunition body is approximatively regarded as a rigid body and the decelerating parachute is approximatively regarded as a particle in this paper because the motion of the terminal-sensitive submunition body needs to weightily study in the deceleration and dispinning stage, On that basis, the particle-rigid body dynamics model is founded.

2. Basic Hypothesis

(1) The acceleration of gravity g is constant, and the curvature influence of the earth is ignored.

(2) The drag index of the parachute and the mass of parachute (including the additional mass) are all constants, the distance between the joint point and the center of mass is changeless, and the moment of inertia of the parachute is ignored.

(3) The canopy of the parachute is an axially symmetric body, the joint line between the parachute and the body is superposition to the axis of symmetry.

(4) The mass of the parachute cords is divided into two pieces and is fell under the body and the parachute, the distortion and torsional force are ignored.

(5) The tensile force and the rolling moment are at the same line with the direction of the body speed but the opposite direction.

3. Coordinate Systems

Firstly, the ground inertial coordinate system $O_0 - XYZ$ is founded. The origin O_0 is the ground projection point of the submunition's dispensing point, the axis O_0X is horizontal and follows the direction of the speed, the axis O_0Y follows the plumb line, and the axis O_0Z is determined by the right hand rule.

Then, the parallel motion coordinate system $O - XYZ$, the body axis coordinate system $O - X_1Y_1Z_1$, the speed coordinate system $O - X_2Y_2Z_2$ and the relative speed coordinate system $O - X_rY_rZ_r$ can be founded in turn. The origin O is the mass center of the submunition, the axis OX_1 is superposition to the body axis and follows the direction of the speed, the axis OY_1 plumbs the axis OX_1 , and the axis OZ_1 is determined by the right hand rule. The axis OX_2 is superposition to the direction of speed, the axis OY_2 plumbs the axis OX_2 , and the axis OZ_2 is determined by the right hand rule. The axis OX_r is superposition to the direction of relative speed v_r , the axis OY_r plumbs the axis OX_r , and the axis OZ_r is determined by the right hand rule. If the wind speed v_a is not considered, the relative speed coordinate system $O - X_rY_rZ_r$ can be regarded as the speed coordinate system $O - X_2Y_2Z_2$.

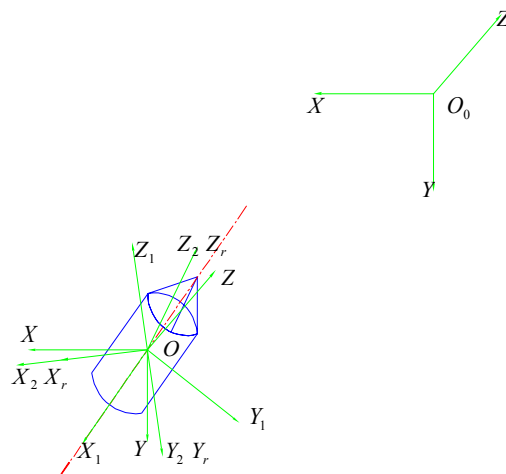


Figure 1 Coordinate systems of parachute-submunition system

4. Forces and moments

Before modeling, the body and the correlative parachute cords are regarded as the whole body; the parachute and the residual correlative parachute cords are regarded as the whole parachute.

Actually, there are only pull force and minim elongation when the parachute cords draws straight. For making the dynamics model be close to the fact, the parachute cords are treated with a pull force spring. Finally the parachute cords force is regarded as the single degree-of-freedom simple harmonic wave.

$$T = K_e \Delta l_p + c \dot{\Delta l}_p$$

K_e is the spring rigidity, c is the damping coefficient of the spring, Δl_p is the elongation of the parachute cords.

The forces of parachute-submunition system can be denoted with the following picture:

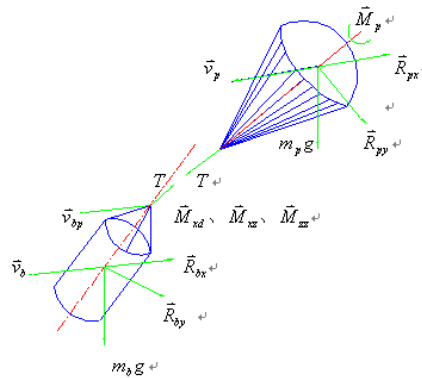


Figure 2 Forces and moments of parachute-submunition system

4.1. Forces and moments of the Parachute

The forces and moments of the decelerating parachute includes the aerodynamic resistance \bar{R}_{px} , the parachute cords pull force \bar{T} and the rolling moment \bar{M}_p .

The aerodynamic resistance \bar{R}_{px} is the part of aerodynamic force that follows the direction of relative speed; its direction is opposite to the relative speed.

$$R_{px} = \frac{1}{2} \rho v_p^2 C_{px} S_p$$

The parachute cords pull force \bar{T} is along the decelerating parachute axis, its projection in the parallel motion coordinate system is:

$$\bar{T} = \begin{bmatrix} T_x \\ T_y \\ T_z \end{bmatrix} = K_e \frac{\Delta l_p}{r_p} \begin{bmatrix} x_p \\ y_p \\ z_p \end{bmatrix} + c \frac{\Delta \dot{l}_p}{r_p} \begin{bmatrix} v_{px} - W_x \\ v_{py} \\ v_{pz} - W_z \end{bmatrix}$$

$r_p = \sqrt{x_p^2 + y_p^2 + z_p^2}$, Δl_p is the elongation of the parachute cords, (x_p, y_p, z_p) is the mass center coordinate of the decelerating parachute.

The rolling moment \bar{M}_p is the moment that made the parachute rotating, and its direction is along the parachute axis.

$$M_p = \frac{1}{2} \rho v_p^2 S_p l_p m_{xw}$$

4.2. Forces and moments of the Body

The forces of the body are projected onto the parallel motion coordinate system, and the moments of the body are projected onto the body axis coordinate system.

The aerodynamic resistance \bar{R}_{bx} is the part of aerodynamic force that follows the direction of the body's mass center speed; its direction is opposite to the direction of the body's mass center speed.

$$R_{bx} = \frac{1}{2} \rho v_r^2 C_{sd} S_d.$$

The aerodynamic \bar{R}_{by} plumbs the relative speed in the relative attack angle plane, its direction is the attack angle direction.

$$R_{by} = \frac{1}{2} \rho S_d C'_y v_r^2 \delta_r.$$

Besides, the forces of the body also includes gravity \bar{G} , the parachute cords pull force \bar{T} , the static moment \bar{M}_{xd} , the polar damping moment \bar{M}_{xz} , the equatorial damping moment \bar{M}_{zz} .

$$\bar{M}_{xd} = \frac{1}{2} \rho v_r^2 S_d L m'_{xd} (\bar{I} \times \bar{X}) \delta_r / \sin \delta_r \quad M_{xz} = -J_x k_{xz} v_r \dot{\gamma}$$

$$M_{zz} = -J_y k_{zz} v_r \dot{\phi}$$

In addition, the rolling moment of parachute \bar{M}_p can impact the body's motion.

$$\bar{M}_p = \frac{1}{2} \rho v_p^2 S_p l_p m_{xw} \times [L_2] \times \bar{I}_p$$

\bar{I}_p is the unit vector in the direction of the parachute axis.

$$\bar{I}_p = \frac{(\bar{r}_p - \bar{r}_{bp}) / L}{L} = \begin{bmatrix} (x_p - x_{bp}) / L \\ (y_p - y_{bp}) / L \\ (z_p - z_{bp}) / L \end{bmatrix}, \quad L = \sqrt{(x_p - x_{bp})^2 + (y_p - y_{bp})^2 + (z_p - z_{bp})^2}$$

5. Dynamics Models

5.1. Motion Equations of the Parachute

According to the momentum theorem:

$$m_p \frac{d\bar{v}_p}{dt} = \bar{G} + \bar{R}_{px} + \bar{T}$$

The motion equations of the parachute can be founded as follows:.

$$\begin{cases} \frac{dv_{px}}{dt} = \frac{1}{m_p} \left(-\frac{1}{2} \rho v_p C_p S_p v_{px} + T_x \right) \\ \frac{dv_{py}}{dt} = \frac{1}{m_p} \left(m_p g - \frac{1}{2} \rho v_p C_p S_p v_{py} + T_y \right) \\ \frac{dv_{pz}}{dt} = \frac{1}{m_p} \left(-\frac{1}{2} \rho v_p C_p S_p v_{pz} + T_z \right) \end{cases}$$

According to the kinematics equation:

$$\frac{d\bar{r}_p}{dt} = \bar{v}_p$$

The following equations can be founded as follows:

$$\begin{cases} \frac{dx_p}{dt} = v_{px} \\ \frac{dy_p}{dt} = v_{py} \\ \frac{dz_p}{dt} = v_{pz} \end{cases}$$

5.2. Motion Equations of the Body

According to the momentum theorem

$$m \frac{d\vec{v}}{dt} = \sum F_i$$

The motion equations of the body can be founded as follows:

$$\left\{ \begin{aligned} \frac{dv_x}{dt} &= -\frac{1}{m} \left[\frac{1}{2} \rho v_r S_d C_{xd} (v_x - W_x) + \frac{1}{2} \rho v_r^2 S_d C'_y \delta_r \right. \\ &\quad \left. (\sin \theta_r \cos \Delta + \sin \psi_r \cos \theta_r \sin \Delta) - T_x \right] \\ \frac{dv_y}{dt} &= \frac{1}{m} \left[-\frac{1}{2} \rho v_r S_d C_{xd} v_y + \frac{1}{2} \rho v_r^2 S_d C'_y \delta_r \right. \\ &\quad \left. (\cos \theta_r \cos \Delta + \sin \psi_r \sin \theta_r \sin \Delta) + T_y \right] + g \\ \frac{dv_z}{dt} &= \frac{1}{m} \left[-\frac{1}{2} \rho v_r S_d C_{xd} (v_z - W_z) + \right. \\ &\quad \left. \frac{1}{2} \rho v_r^2 S_d C'_y \delta_r \cos \psi_r \sin \Delta + T_z \right] \\ \frac{dx}{dt} &= v_x \\ \frac{dy}{dt} &= v_y \\ \frac{dz}{dt} &= v_z \end{aligned} \right.$$

According to the absolute momentum moment theorem of the relative mass center:

$$\frac{d\vec{H}}{dt} = \frac{d\vec{H}}{dt} + \vec{\Omega} \times \vec{H} = \sum M$$

The rotate equations can be founded:

$$\left\{ \begin{aligned} \frac{d\gamma}{dt} &= \dot{\gamma} \\ \frac{d\varphi_1}{dt} &= \dot{\varphi}_1 \\ \frac{d\varphi_2}{dt} &= \dot{\varphi}_2 \\ \frac{d\dot{\gamma}}{dt} &= -k_{xz} \dot{\gamma}_r - \frac{J_y}{J_x} k_{zz} v_r \dot{\varphi}_1 \sin \varphi_2 + \frac{\rho v_p^2 S_p l_p m_{xw}}{2LJ_x} [(x_p - x_{bp}) \cos \varphi_1 \cos \varphi_2 \\ &\quad - (y_p - y_{bp}) \sin \varphi_1 - (z_p - z_{bp}) \cos \varphi_1 \sin \varphi_2] - \dot{\varphi}_1 \sin \varphi_2 - \dot{\varphi}_1 \dot{\varphi}_2 \cos \varphi_2 \\ \frac{d\dot{\varphi}_1}{dt} &= \frac{\rho v_r^2 S_d l m'_{sd} \delta_r}{2 \sin \delta_r J_y \cos \varphi_2} (\cos \alpha \sin \delta_{r1} + \sin \alpha \sin \delta_{r2} \cos \delta_{r1}) - k_{zz} v_r \dot{\varphi}_1 - \dot{\varphi}_1 \dot{\varphi}_2 \\ &\quad + 2\dot{\varphi}_1 \dot{\varphi}_2 t g \varphi_2 + \frac{\rho v_p^2 S_p l_p m_{xw}}{2LJ_y \cos \varphi_2} [(x_p - x_{bp}) \sin \varphi_1 \cos \varphi_2 - (y_p - y_{bp}) \cos \varphi_2 \\ &\quad - (z_p - z_{bp}) \sin \varphi_1 \sin \varphi_2] \\ \frac{d\dot{\varphi}_2}{dt} &= \frac{\rho v_r^2 S_d l m'_{sd} \delta_r}{2 \sin \delta_r J_y \cos \varphi_2} (-\sin \alpha \sin \delta_{r1} + \cos \alpha \sin \delta_{r2} \cos \delta_{r1}) - k_{zz} v_r \dot{\varphi}_2 + \\ &\quad \frac{\dot{\varphi}_1 \cos \varphi_2}{J_y} (J_x \dot{\gamma} + J_x \dot{\varphi}_1 \sin \varphi_2 - J_y \dot{\varphi}_1 \sin \varphi_2) + \frac{\rho v_p^2 S_p l_p m_{xw}}{2LJ_y} [(x_p - x_{bp}) \sin \varphi_2 \\ &\quad + (z_p - z_{bp}) \cos \varphi_2] \end{aligned} \right.$$

6. Simulation results

Given the initial conditions: $v_0 = 883m/s$, $h_0 = 2000m$, $\theta_0 = -48^0$

After the simulation of the freely falling stage, the motion of the deceleration and dispinning stage can be computed. On the base of the Figure 3 and the Table 1, we can see, the speed of the terminal-sensitive submunition has been decelerated from 883m/s to 63.66m/s in 7.5 second flight, and the height of the terminal-sensitive submunition has been descended from 2000m to 494.214m in 7.5 second flight. The results can be provided to the stable scanning equipment design of the terminal-sensitive submunition.

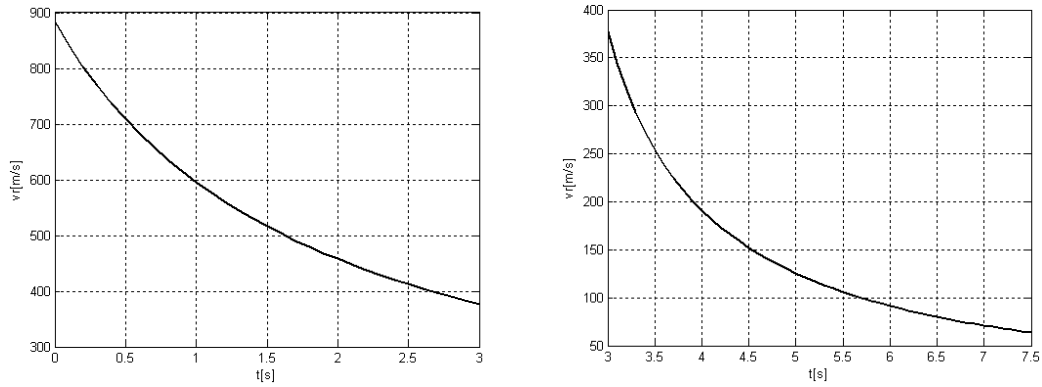


Figure 3 The curve of speed v in the freely falling stage and the deceleration and dispinning stage

Table 1 Part of ballistics results in the deceleration and dispinning stage

t [s]	v [m/s]	y [m]
7	71.059	506.46
7.1	69.453	503.73
7.2	67.913	501.143
7.3	66.436	498.697
7.4	65.019	496.388
7.5	63.66	494.214

7. Conclusion

This paper roundly analyzes the forces and moments of the terminal-sensitive submunition in the deceleration and dispinning stage. On that basis, the particle-rigid body dynamics model is established. The model can be used to compute and simulation. It can provide the overall design and the stable scanning equipment design of the terminal-sensitive submunition with some helpful references, and can be used to the exterior ballistic of terminal-sensitive submunition.

8. References

- [1] Rui Guo, Rongzhong Liu, et al., *The simulation of target sensitivity projectile trajectory based on MATLAB/Simulink*, Journal of Projectiles, Rockets, Missiles and Guidance, 5(2005)4.
- [2] Liu Rongzhong, *Study of the structural dynamics response and efficiency analysis about terminal-sensitive projectile*, Doctorial Paper[D], 1996.
- [3] Qiren Yang, *Flight Dynamics of Cargo Projectile*, National Defense Industry Publishing House. 93-140, 1999.
- [4] Dayao Li, *Motion equations of object-parachute system with particle-rigid body method*, Return and Remote Sensing of Spaceflight, 16(1995)3.
- [5] Ruce Wang, Rongzhong Liu, et al., *Structure and function of smart ammunition*, Weaponry Industry Publishing House, 2001.
- [6] Jingrong Shu, Zipeng Han, et al., *Study on realizing stable scanning of target sensitivity projectile by using strong-asymmetric mass and aerodynamic of projectile body*, Fire Control & Command Control, 28(2003)3.
- [7] Mingyu Cong, Chenxun Shao, et al, *The dynamics model for the trajectory of low-altitude parachute-bomb (LAPB)*, Journal of Ballistics, 12(2000)1.
- [8] Kun Huang, Rongzhong Liu, *Optimal design of system efficiency parameters about the terminal-sensitive projectiles based on neural net work and genetic algorithm*, AC